SUPPLEMENTAL DATA

Supplemental Figure 1

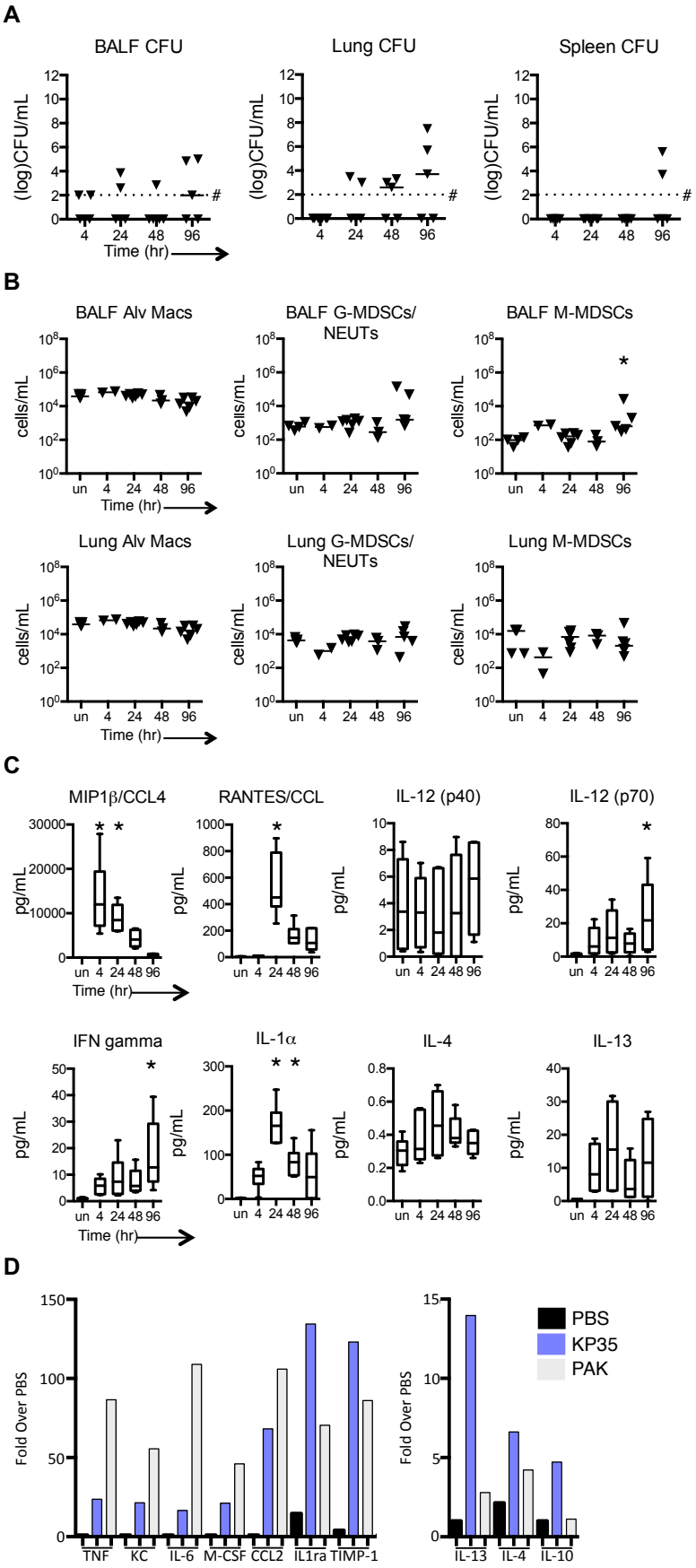

Supplemental Figure 1. The kinetics of KPPR1 clearance, and chemokine/cytokine production in response to KP35.

C57BL/6J mice were infected following inoculation with a non-lethal dose of KPPR1 (10^2 CFU) as previously described and bacterial clearance was followed over 4 days (Poe, et al., 2013,Tzouvelekis, et al., 2013).
(**A**) KPPR1 recovery from bronchoalveolar lavage fluid (BALF), lung homogenate and spleen following intranasal inoculation of 1-2 x 10^2 CFU to WT C57BL/6J mice over the course of a 4 day infection. # = the lower limit of detection.
(**B**) Cellular response to infection in BALF and lung homogenate determined by flow cytometry – Resident alveolar macrophages (Alv Macs), Granulocytic-myeloid derived suppressor cells (G-MDSCs/NEUTs) and monocytic-MDSCs (M-MDSCs). Horizontal lines represent median values and each point represents an individual mouse; data were compiled from 2 independent experiments. *p<0.05, as compared to uninfected control (un), Kruskal-Wallis test, one-way ANOVA, Dunn's correction for multiple comparisons.
(**C**) Selected cytokine and chemokine content (see Figure 2) of BALF of WT mice following intranasal inoculation of 1-2 x 10^8 CFU of KP35 to WT mice over the course of a 4 day infection was quantified by multiplex assay, N=6). For data presented as box-and-whiskers plots, horizontal lines indicate the median, boxes indicate 25th to 75th percentiles, and whiskers indicate minimum and maximum values of the data set; data were compiled from 2 independent experiments. *p<0.05, as compared to uninfected control (un), Kruskal-Wallis test, one-way ANOVA, Dunn's correction for multiple comparisons.
(**D**) Comparison of responses to KP35 and *P. aeruginosa* (PAK) (10^7 CFU) by semi-quantitative cytokine array of pooled BALF (N=3) from infected WT C57BL/6J mice harvested at 24 hours. A lower inoculum was used due to the lethality of 10^8 CFU of *P. aeruginosa* in this mouse model of pneumonia.

Supplemental Figure 2

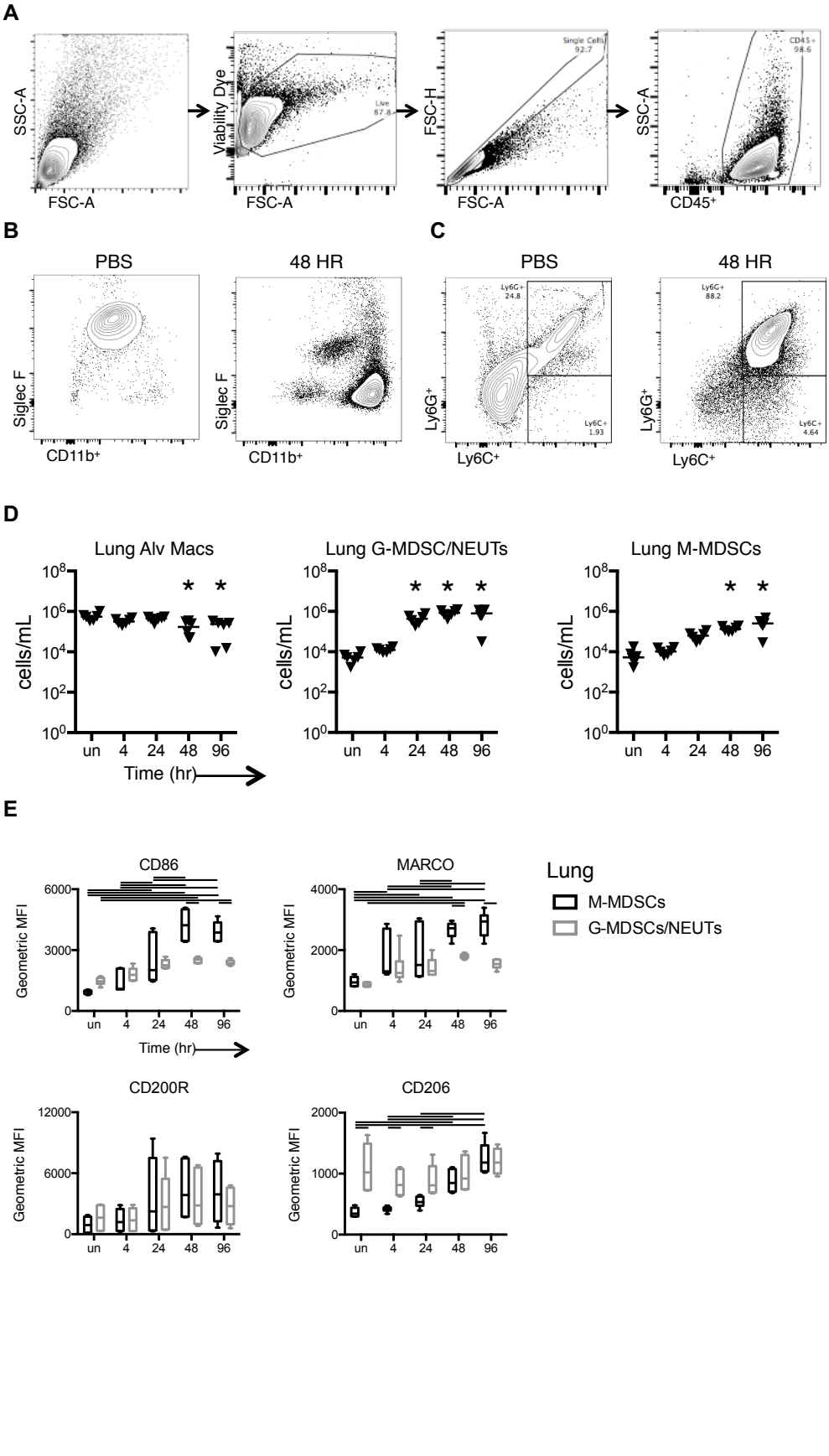

Supplemental Figure 2. Gating strategy for the identification of alveolar macrophage and Ly6C/G populations and immune cell populations in response to KP35 infection. Representative flow cytometric plots of key immune cell populations recovered from BALF of WT C57BL/6J mice given either PBS or KP35 (10^8 CFU) at 48 hours using multicolor flow cytometry. (**A**) $CD45^+$ populations were first gated out after identifying viable singlet cells. (**B**) Resident alveolar macrophages (Alv Macs) were identified as $SiglecF^+$ and $CD11b^{lo\text{-}mid}$ as previously described (Misharin, et al., 2013). (**C**) Remaining $CD11b^+$ cells were plotted Ly6C versus Ly6G to identify G-MDSCs/NEUTs ($CD45^+CD11b^+MHCII^{lo}Ly6C^{hi}Ly6G^{hi}$) and M-MDSCs ($CD45^+CD11b^+MHCII^{lo}Ly6C^{hi}Ly6G^{lo}$) as previously described (Penaloza, et al., 2015). Absolute numbers of immune cell populations were calculated using uniform dyed microspheres. (**D**) Enumeration of macrophage/monocyte populations in the KP35 infected LUNG homogenate; Alv Macs, G-MDSCs/NEUTs and M-MDSCs cells by flow cytometry. Lines represent median values. Each point represents an individual mouse; data were compiled from 2 independent experiments. *p<0.05, as compared to uninfected control (un), Kruskal-Wallis test, one-way ANOVA, Dunn's correction for multiple comparisons. (**E**) Comparison of the geometric MFI of surface markers associated with the M-MDSCs and G-MDSCs/NEUTs cells in lung homogenate by flow cytometry (N=6). For data presented as box-and-whiskers plots, horizontal lines indicate the median, boxes indicate 25th to 75th percentiles, and whiskers indicate minimum and maximum values of the data set Horizontal bars represent p<0.05, two-way ANOVA, Bonferroni's correction for multiple comparisons.

Supplemental Figure 3

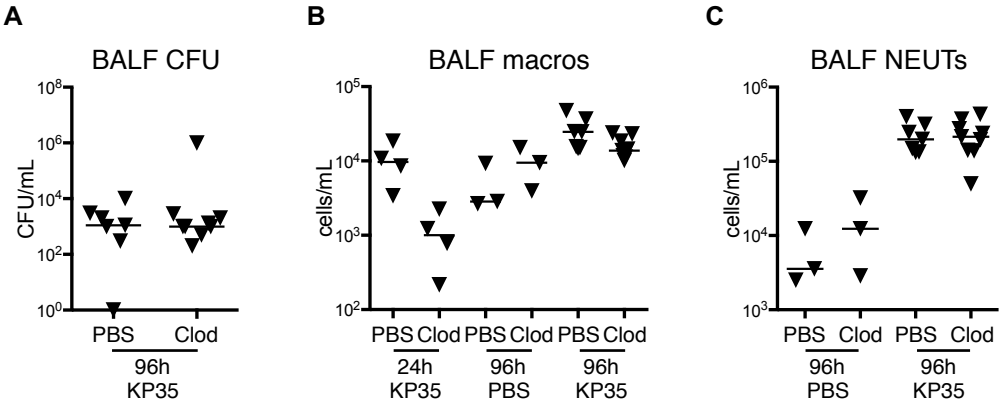

Supplementary Figure 3. Depletion of alveolar macrophage population does not affect KP35 clearance.
Airway macrophages were depleted from WT C57/BL6J mice by administration of 75 µL clodronate as compared with PBS loaded liposomes intranasally as previously described (Martin, et al., 2011), and infected 24 hours later with KP35 (10^8 CFU) or a PBS control.
(**A**) KP35 recovery enumerated from BALF at 96 h post infection in mice pre-treated with liposomes.
(**B**) Macrophages/monocytes (**macros**) ($CD11c^+/MHCII^{low\text{-}mid}$) were depleted by 1 log at 24 hours post administration of PBS, with no difference in macrophage/monocyte populations between clodronate and PBS liposome treated groups at 96 hours. (**C**) Neutrophils (**NEUTs**) ($Ly6C/G^+/MHCII^-$) were enumerated by flow cytometry at 96 hours of infection. Horizontal bars represent $p<0.05$ Kruskal-Wallis test, one-way ANOVA, Dunn's correction for multiple comparisons.

Supplemental Figure 4

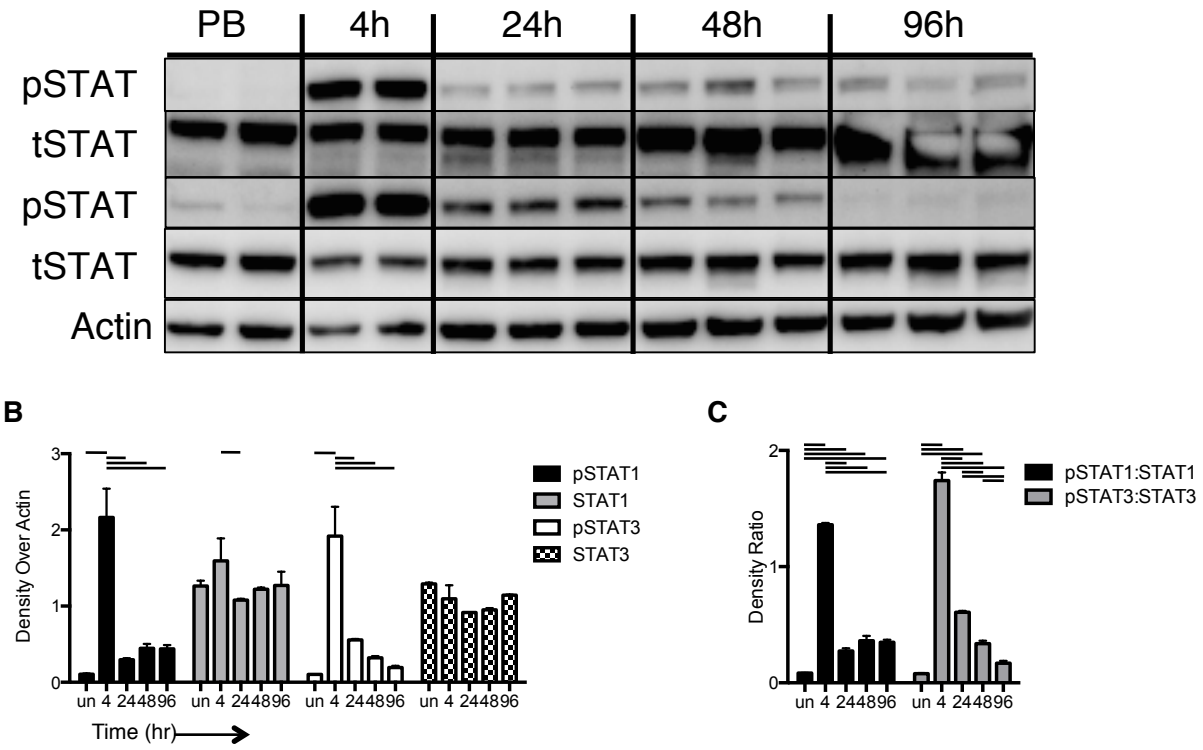

Supplemental Figure 4. Kinetics of STAT1/3 activation following KP35 infection.
(**A**) Immunoblots of lung lysates obtained from 3 individual mice are shown at the designated intervals following KP35 infection, with (**B**) densitometry normalized to actin and (**C**) ratios of phosphorylated proteins to total protein. The brisk activation of JAK/STAT signaling as a response to lung infection is demonstrated by phosphorylated STAT1 and STAT3 at 4 hours but are differentially attenuated over the course of infection. For (**B**) and (**C**), data presented as box-and-whiskers plots, horizontal lines indicate the median, boxes indicate 25th to 75th percentiles, and whiskers indicate minimum and maximum values of the data set horizontal bars represent, $p<0.05$, two-way ANOVA, Bonferroni's correction for multiple comparisons, representative of 2 independent experiments.

Supplemental Figure 5

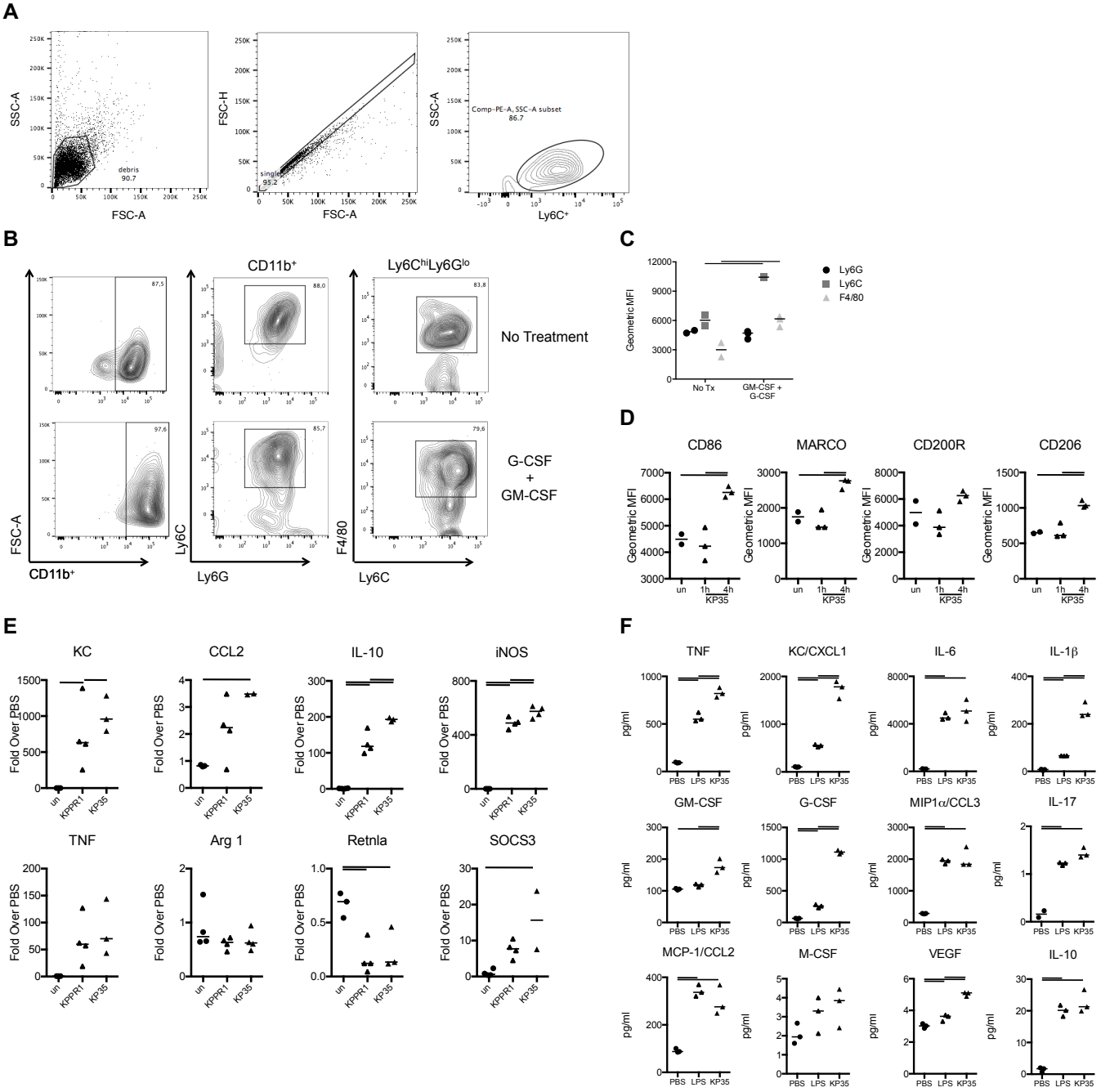

Supplemental Figure 5. M-MDSC like properties of in vitro polarized MDSCs derived from murine BM cells (BM/MDSCs). Characterization of Ly6C$^+$ cells isolated from lung or bone marrow.

(**A**) Cells isolated from the BM and BALF of uninfected (un), *E. coli* LPS 50 µg or KP35 10^8 CFU intranasally for 48 hours. Total Ly6C$^+$ cells were isolated by positive selection after incubation with Ly6C$^+$-PE, and PE-labeled magnetic beads (Fig. 3F). Flow cytometry was performed on isolated cells to confirm purity of cells isolated. Mononuclear cells were isolated from BM of WT C57BL/6J mice and polarized to M-MDSC phenotype as previously described (Marigo, et al., 2010). Cultured BM/M-MDSCs showed (**B,C**) increased expression of F4/80 and Ly6C after polarization with G-CSF and GM-CSF (N=3), as well as (**D**) increased expression of CD86, MARCO and CD206 after 4 hours of incubation with KP35 (N=3). (**E**) Quantitative RT-PCR was used to measure gene expression of KC, CCL2, IL-10, iNOS, TNF, Arginase- 1 (Arg1), Retnla, SOCS3 (N=4). (**F**) Cytokine levels in the supernatant collected from cultured cells stimulated with LPS or KP35 (MOI 10) for 4 hours. Pro-inflammatory cytokines TNF, KC/CXCL1, Il-6, IL-1β and granulocyte/monocyte associated cytokines GM-CSF, G-CSF, MIP1α/CCL3, IL-17, MCP-1/CCL-2, M-CSF were increased in response to infection with KP35. M-MDSC associated cytokines VEGF and IL-10 were also increased (N=3). For all graphs, each dot represent a biologic replicate, horizontal lines are median values. Horizontal bars between groups represent $p<0.05$, two-way ANOVA, Bonferroni's correction for multiple comparisons. Representative graphs of 2 independent experiments.

Supplemental Figure 6

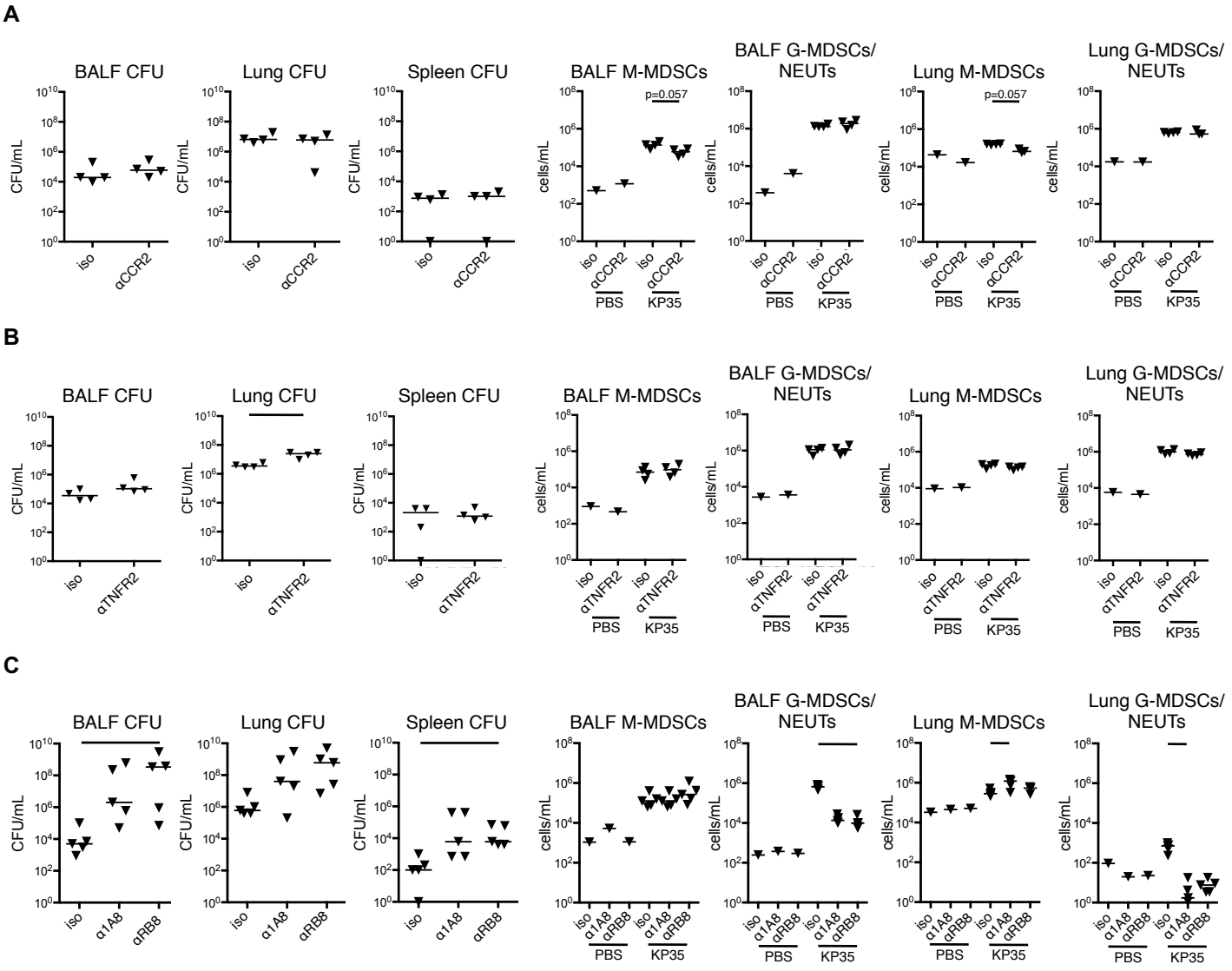

Supplemental Figure 6. Consequences of targeted MDSC depletion strategies.
WT C57BL/6J mice were given antibodies prior to and/or at the time of inoculation 10^8 CFU of KP35 and the effects on MDSC populations by flow cytometry (as described in Supplemental Figure 1) and bacterial clearance were quantified at 48 hours.
(**A**) Anti-CCR2 (αCCR2) at the time of infection (Xiong, et al., 2015), resulted in a very modest reduction in the M-MDSC population and had no effect on KP35 clearance at 48 hours.
(**B**) TNFR2, reported to selectively promote M-MDSCs proliferation (Polz, et al., 2014) (Hu, et al., 2014) was targeted with anti-TNFR2 (αTNFR2) given at 24 h prior and on the day of infection with KP35. Significant depletion of the $Ly6C^+$ population was not achieved, but recovery of KP35 from the lungs was significantly increased at 48 hours, consistent with the anti-inflammatory effects of TNFR2 blockade.
(**C**) Mice pretreated with anti-Ly6G (α1A8) or anti-Ly6C/G (αRB8) (Schumak, et al., 2015) at the time of infection had the expected diminution of both $Ly6C^+$ and $Ly6G^+$ cells at 48h post infection and increased recovery of KP35 from BALF and lung. Horizontal bars represent $p<0.05$, Kruskall-Wallis test, one-way ANOVA, Dunn's correction for multiple comparisons.

SUPPLEMENTAL TABLES

Supplemental Table 1

Parameters	KP35
Total No. of Reads	3019946
Total No. of Bases	377493250
Total length (bases)	5502691
No. of Contigs	123
Average Contig size (bases)	44612
N50 Contig size (bases)	137176
Largest Contig size (bases)	339355
Chromosome length(bp)	5205019
Coverage depth	69

Supplemental Table 2

KP35 special OGs	OG group number	Annotation label	Annotation	Protein length (aa)	Protein seq
Group1	OG5_215184	fig|6666666.145384.peg.1015	Arginine/ ornithine antiporter *ArcD* CDS	332	MWVDYAKAFGIILVVFGHVNRGLFNSGIFTTEIYHSLDNVIYSFHMPLFFFLSGLFFIESISGKSKIRFISGKFKTIFYPYAVWSILQGCIEVFLSNYTNSKTSLISVLSFPFHPRAQFWFLYALLLIFILSAVIYNKFFTKIIPLLLVFSFFSYIYGEDVISIYYINYIDNNIVFFFLGCLVYKYNAYLKDVLNIYSFIILTVVFVLVEYFYFVRLGNDYSELNFTTAAIAIVGIFWISNLSVVLSKYNVAWLSHLGRQSIIIFLVHILASSGVRIVLTKLFHIENWYFNIISGTVAGIILPLLFYHFALRLKMSFFFVYPYVKTPSNLK
Group2	OG5_245758	fig|6666666.145384.peg.2682	probable terminase large subunit CDS	464	MAEIILPANNWTPRPHQRRAWAEIQGGKKRAALCWPRRYGKDDFSLHMTACKAFERVGNYAHCLPQANQVRKAIWKAVNPRTGRLRIDEAFPHELRRKTLDNEMMIEFINGSTWQAVGSDNYGALIGSGHVGIVFSEWALSNPSAWAFLRPILADNGGWAFFVSTPRGKNHFYKMFQGGLKDPENWFCDHLSADITGHIPPETLAQELREMQAERGEEEGLALFNQEYMCDWNAAVPGAYYSSILVGLEKAGQIGNVPWDPQYEVYTSWDLGIGDATAIWFYQFIGKEVRVIDYYESSGVGLEHYVKILREKPYTYAERHFFPHDVRARELSTGASREETLGKLGMRCKVLPATSVDDGISEVRMMLRSCWFDKTKCEKGLEALGQYQKEWDDTRKMYKPTPLHNWTSHGADSFRYGAVGSKSLRSGNRHTTQQFAQSNYDPYNPPGHSQQFYADSDWDLYGDN
Group3	OG5_198600	fig|6666666.145384.peg.2699	hypothetical protein	148	MENIEELKREIFSWAAESGQELVAIEISRMWFRLGGNTGVLKLHQIEDADGKADWRAINNNRQQIFRWLRGETKAAITKTQALAKAMEAALPAERYARLDMSTQYLICVAIREFAAAIIALLLEARDGPQQVAKALQAMRETQRLTSV

Group4	OG5_191549	fig|6666666.145384.peg.2702	hypothetical protein (prophage related)	188	MTSTTAIAIAADMSKLQALLENEDGSGLSAEMIADTMEGLELQLGDKLDAVFVHVRNLEGLAKTCDEEAKRLAARKKSFEGKITNLKNYVLQCLLAAGKDTVKTAKNTFTARKGAINVVIDNVDLLPDDLVTVETVVTPDKKAIKEAIESSQAAAAQITADGGEIPGELLNPVPGAHLEIGERSLQVR

Supplemental Table 2 – Four KP35 special OGs which are not present in ATCC KPPR1 and NJST258-1
KP35 contained four unique OGs and each of these consisted of only one protein. The first OG included the arginine/ornithine antiporter *arcD* CDS. BLASTP indicated that the 332 aa length *ArcD* protein is also present in *K. pneumoniae* strains such as UHKPC4, UHKPC23, MGH45, and BIDMC 18C. The former two were isolated in Midwestern U.S. hospitals. The second OG consisted of a probable terminase large subunit CDS. Homologs of this 464 aa length protein were found in multiple species, such as *K. oxytoca*, Enterobacteriaceae and *Kosakonia radicincitans*. However, limited information is known about its function. The remaining two OGs consisted of hypothetical proteins.

Supplemental Table 3

OG group numbers	Representative protein within the OG	Annotation	Protein seq
OG5_164793	KPNJ1_00785	Transglycosylase SLT family protein CDS	MVARRVLMFLLLFPPLACAQSIPSGYRQIAEQENVPA EALYSLALTESAKKLAHGVRPWPWTINVAGIGYRYAS RDEAYQALLGFIRRYPLKRIDVGVAQVNLGWNGSRFS SYWHAFDPYTNLRVAARILRECYDAQPGSWMQAAG CYHHPAGGKPARVYKAVVQRHLNTLNPVKPTAVSWV EPKRKTP
OG5_245711	KPNJ1_00800	Superfamily I DNA helicase CDS	MMFSLFTREKAAAPVPQAEEKAVLKPSLRKSGKLKIS DEQARYHREPPLIDYLPWVEYLPSSQSILLDDGVSVG AVFDVLPVGSEGRTAERLEEIRDVIEDAIQDSFDERDT CPWVIQFFCQDETDVTAYLDRLRGYIKPWAQGSAFTE DYLREIEGHMRGIAVPQGLFIDKTVTGAPWRGQQRRT RMVVYRYVDPAQRDPYSPETALSQVCERLVSALNGA GVVAERQSGEQIHAWLLRWFNPDPQWVEKEVLYRT ARHHDNPHNALPLMTDFSESLWFTPPRSDAENGVW WFDEQPHRAVTIDRLRRPPAVGHLTGETRKGDNINAL MDLMPEGTVMCMTIVVQAQDVLEERFTHLAKNAIGEN VESSRVREDAAIAKSFLGERHKLYHGSMTFLLTAPDL PQLQSRQRELNAVLLNAGLQPTRGEYEVAPLNGYLR AMPMCFNPARDKHHWYTRLTFVQHLANLSPLFGRDT GTGNPGFTFFNRGGAPLTFDPLNSNDRTKNAHMAIF GPTGSGKSATLNSLFSQLMAIHRPRLFIAEAGNSFGLF ADYCGELGLTVNKISIKPGCGISLAPFADAHKLIEQPVV PVSESELSDGIDIDDVDGEEDGDEERDILGELEIAARL MITGGEEKEEARLERADRGMMREAILAAAQQAWDEG RQMITGDLQSAFYQFARDPARPAERQVRAQNMGESL GVFMQGFLGELFNRPGENWPEADVTLIDLGTLAREG YEAPLAVAYISLVNTINNLAERDQFDDREIVFATDEAH MITTNPLLAPYVVKVVKMWRKLGAWLWLATQNLDDF PNAAKKMLNMIEWWLCLVMPPEEVEQIARFKKLTEEQ KAMLLSANKAKHCYTEGVVLASRIEALFRAVPPSLYLA LGMTEKEEKAQRRALMNEYGISELGAAKRVARQMDE LRGILR
OG5_134571	KPNJ1_05495	Ribonuclease P protein component CDS	MVKLAFPRELRLLTPSHFTFVFQQPQRAGTPQITILGR LNSLGHPRIGLTVAKKNVKRAHERNRIKRLTRESFRLR QHELPPMDFVVVAKRGVADLDNRALSEALEKLWRRH CRLARGS
OG5_216139	KPNJ1_00766	ATPase involved in chromosome partitioning CDS	MQVISIISTKGGEGKSTHAANLSGFLADAGLKTLLIDG DYAQPTASSYYSLRYEAPCGLYELLMQTVDLNAPEQII SHTSVSNLDLIVSNDPHEQLKTSMMHAPDGRIRLRNL LQHPLFNAYDVVVIDSQGARSIMLELVLLATNHTALAM IKPVVPDVREFLRGTIPLLEGLLPYRGFGIVLPPVKVLV NCMDYTTLAKDALEALSNIIAEGSYSSADISVSLLDTHI YDLDVYKTGHSLGQPAHRLEYHTDRKSLPAARTMHD LACELFPEWVERFASVLQVQPKGDK

OG5_245694	KPNJ1_00767	Replicative DNA helicase CDS	MAIRFCWYLPASYNSCIRRWGRYPMNNAQRLLPPHSI ESEQSVLGGLMLDNDRWDDIATIVSADNFYVRPHQLI FNAMHDLLMQGKPVDLITLSEHLEQRGVLEQVGGFA YLAEMSKNTPSAANIVAYAEYVASYGRQRQLLALGHD IVGQAGDVRTDVAMLIDDIEQRLFAIAEQHEQGGVADL PEAYGQFLDKLEQRCQSQTSVTGTPTGFQDLDEVTS GLQPGDLVLLAGRPSMGKTALGLALCEAALNVNAGP VQVFSLEMPVDQLLARFTAMLGRVPLQHIRSGDLSEN EWGRISSAASCLLSWKDRLLIDDSSYLTPTMLRSRVR KSVRQFGHPALILVDYLQLMRSPGQENRTLEIAEISRA LKSLAKEMRCPVVALSQLNRDLEKRANKRPNNGDLR DSGALEQDADLIMFVYRDEVYDPQTMDKGTAEIIIGKQ RNGPVDTVKVRYQADITRFEDFPSGAYSLGYGRTAE
OG5_210072	KPNJ1_02399	Glycosyl-transferase	MNKINYQIKYIEYLLRKCRTILTNDISFHADRLREISGTY PDLLNPVTLNEKICHRILFIHNPFYTLLADKLLVRQYVE KRTNLIKLIPLVGVYNRVDDIDFDKLPSKFVLKCNHDS GSAVICTDKTNIDPAKVKSKLKLSLKKNMYYTTREWQ YKNIPPVILCEMYLDLFSSKHRNITPEMIRIHCFHGVAC FIEADFTDSDGNEFINVYDRAWNLQPFQMEYPNTPLP VDEPESFHKSVIAAQDLAKEIDYCRVDLMLKGDDIYFS EITLSPKRGKLKITPSIWDAKLGSMWDLSLAKTGSIEP VYSCP
OG5_139380	KPNJ1_02703	Esterase CDS	MVITLPEIQHRRKNTNMWMRNVMSRALIKGAFALCLL FMNSPLLMAQEEGIKNIVLVHGAFADGSCWSAVISLL QERGYHVSAVQNPLTSLRDDVTATERVLERQKGNVL LVGHSWAGAVITQAGNASNVRGLVYLSALVPDSNQS VSDALARFHAPMTGMEADKNGLIWLDEPEFFHQVMA NELSIKKSRQLAAVQQPVAATAFQEKVKEAAWRKKPS WYLITENDNALNPSVQARFAHEAGAHITRIHSDHLSMI SHPEEVAALIVNAAQSIH
OG5_165100	KPNJ1_02756	Hydrolase of the alpha/beta superfamily protein CDS	MESVIIPVSQGGFVAATLWQRHKAKALVIVHPATAVV QGFYKGFAEYLYKRGFSVITYDYRGTGLSKSGRVRH NKNTMSDWIEQDVGCITAWAKARAPGLTLLAIGHSIG GHAVLLSSASTDLRAAVMVASHAGVTSTISQTKEKLR VWCLLRVLGPALCRLFGYMPARRLGLGEDLPAPAML QWGRWSAMPEYFYDDPEWDARQRAGKITLPILVLGF DDDPWANTEAISRLLAPAQNAKIERREIRRADYGLSSI GHMGFFRTRNAEKLWPLVAQWLERHCPDKRRTT
OG5_138624	KPNJ1_02769	Ribosomal-protein-alanine acetyltransferase CDS	MLVQTNRLYLRPVISSDLNDLFKIYGDPATNTFNPAGP YPNIDHAKMVMNRWLDHWQTHSFGNWAISLLTNPEK IIGFGGLGIRNYDDIVINNLGYRLSTEAWGKGLATEFAI YAIKFGFDVIKLTEISAVVRENHLASQKVLQKSGLRYV KEIHDVKDAPPSLLYSISVDEWLRNLEVNASV
OG5_187367	KPNJ1_02770	Transposase CDS	MTAYNRRFGKAPRHDFDVHRPLETDDDLTAFFTWRE PRRVSKSLTVQYDKVLYLIEDNELSRRAIGKYIEVWHY PDGRKELRLNGVVLPYSTYDRLQKIDQGAIVDNKRLG RTLEFIKLVQDKRDNNRSQALPAGDGPSRRRRKPTE KKSQRSLDEDDMLNALKTLQSRSDEIFGTRK
OG5_153239	KPNJ1_02786	Ribokinase CDS	MMSGKVCVFGSFNFDMVARVDRFPVPGESLVACGS MTSAGGKGANQATAALKAGANVHYIGKIGNDTFGHF ARCHLKGVGFNAVTLLVAEEIPTGNALIYVAGNDAEN MIAVDPGANMTVTDDEIAGCIPAIGCADVVLVQLENNL SAIEQVIDAGKQAGALVILNPAPWQPVEHALLRKVDLL TPNATEAGLMTGRRVDSLTAAAEAADVLHAQGARNVI ITLGASGALLSEHGVKSRVPCFPSHPRDTTGAGDAFN GALAARLACGEPLQAAARFAAAYAAVSVEKQGASSL PEYLEAQERLLRAAADYEMA

OG5_138723	KPNJ1_02869	Glycosyl hydrolase (BNR repeat family) CDS	MTVIPPFDGVIRQHQQDEHIAWAMLPCACPQNHAAN LLPLDDGSLMCVWFGGSQEGKADISIWGSRLAPGSD RWSEAVKLCDDPDRSEQNPVLFQAPDNVLWLLWTA QFAGNQDTAIVRYRLSHDGGRSWGAIDTLLDQPGTFI RQPISVMSDGNWLLPVFYCRTEPGEKWVGNNDVSA VKISSDCGKSWRDVAVPESLGCVHMSITPLPDGRLAA FFRSRWADHIWFSQSSDQGESWSAPVPTTLPNNNSS IQATPLDNGELALVFNNMSAAGATERRASLYDEIADD DGRREPEATGKSAFWGAPRAPMTVAISADGGESWP WLRNLDEGDGYCMTNNSEQKLNREFSYPSIKQGADG NLHIAYTWYRQAIKYVRVSPQWVKGESA
OG5_131031	KPNJ1_02871	3-oxoacyl-[acyl-carrier protein] reductase CDS	MKRAMVTGASSGIGAAVVRQLLADSWQVIGMSRSLP PFSQPNFRHLMVDVSQRSALLAALEQIEPPQAIIHAAG SMAAATLGNLDPQRSESLWRLHVDAAQTLVNHFAPT MGPGGRIVLLGSRTSRGAAGRSQYAATKAALVALAR SWAAELAPAGVTVNVVAPGATDTPMLHQPGRESSPP RLPPLGRLITPQEVVSLVSWLLSEGASAMTGQELVMC GGASLG
OG5_173571	KPNJ1_03141	Terminase large subunit CDS	MMATESVTSMTSTLTSKPTLNPVLRSFWTTQARNKVL YGGRSSSKSWDAAGIAIFLSNKYSLRFCCARQIQNKIE ESVYTLLKIQIDRFGLRHRFRILNNKIINRVTGSEFVFY GLWRNIEEIKSLEGISVLWLEEAHALTEYQWKILEPTIR KEGSECWFIFNPGLVTDFVWRNFVVDPPEDTLIRKIN YDENPFLSDTMLKVIEAAKRRDPDGFKHVYEGVPESD DDAAIIKLSWIEAAVDAHKILNFEPSGRKRIGFDVADSG ADKCANVYRHGSVVYWADEWKAKEDELLKSCQRTY QAALERDADIVYDSIGVGASAGAKFSEINEDRKRENM NASRINYQRFNAGAGVNEPDYEYSGIPNKDFFANLKA QAWWLVADRFRNTFNAVKNGEQYPVDELISIDSSCPL LEKLKLELTTPHRDFDKNGRVMVESKKDLAKRDVPSP NVADAFIMAFAPTDTAMDIWEALGNS
OG5_187236	KPNJ1_03315	Fructose-bisphosphate aldolase CDS	MLADIKYWESDAQNKHYAIAHFNVWNAEMLMGVIDA AEESKSPVIISFGTGFVGNTSFEDFSHMMVSMAKKAS VPVITHWDHGRSMEIIHNAWVHGMNSLMRDASAFDF EENIRLTKEAVDFFHPLGIPVEAELGHVGNETVYEEAL AGYHYTDPSQAAEFVERTGCDSLAVAIGNQHGVYTS EPKLNFEVVKRVREAVSVPLVLHGASGISDADIKKAIS LGISKINIHTELCQAAMAAVQENQNQPFLHVEREVRK AVKVRAMEKIKLFGSDGKAE
OG5_184976	KPNJ1_01308	Terminase, endonuclease subunit CDS	MSLSPARQHRLRVQAEQAARQGGSVRHASGYDLML LQLAEDRRRLKGVQSTVKKAQIKVELLPKYTAWADGV LAAGGAQQDDVLMFLMVWRIDAGDFAGGLQIAAHAL KHGWVMPQALGRRNVQTVVAEELADQAEAAQRMKA EFPADVLLQALSLTDALDMPDQSRARLHKAIAAVISES RPAAALNHYTFALQLDPRCGVKKDKERLERHLRNSH
OG5_184979	KPNJ1_01305	Terminase, ATPase subunit CDS	METMTPAELDPRRQALLLYFQGYRIARIAEMLGEKAA TVHSWKKRDKWGSYGPLDQMQLTTAARYCQLIMKE QKEGKDFKEIDLLARQSERHARIGKFNNGGNEADLNP NVENRNRGPRKPPEKNLFSDKQIEKLEEIFRAGMFEY QRHWWEAGIKHRIRNVLKSRQIGATYYFAREALIDALV TGRNQIFLSASKAQAHVFKQYIIEFAKEVDVELKGDPM VLPNGATLYFLGTNARTAQSYHGNLYLDEYFWIPKFQ ELRKVASGMALHKKWRQTYFSTPSSLTHSAYPFWSG ALYNRGRSKTDRVDIDLTHSALAAGLLCADGQFRQIV TVEDAVRGGCNLFDLDQLRLEYSPDEYQNLLMCEFID DLASVFPLSDLQACMVDSWEVWEDFHALALRPFGW GEVWIGYDPAKGTQNGDSAGCVVITPPSVPGGKFRIL ERHQWRGMDFRAQAEAIRQLTLQYNVTYIGIDSTGVG HGVYENVKGFFPAVREFVYNPNVKNALVLKAYDIISH RRIEFDAGHTDIAQSFMAIRRATTASGNRPTYEASRS

			EEASHADLAWATMHALFNEPLQGEAANTSNIVEIF
OG5_133244	KPNJ1_03993	Gluconate 5-dehydrogenase CDS	MKRINIMIGKDFAQHLFSLRDRVAFVTGAGSGIGQTIA CSLASAGARVVCFDLRDDGGLAETVSHIESIGGQACS YNGDVRQIADLRAAVALAKSRYGRLDIAVNAAGIANA NPALEMESEQWQRVIDINLTGVWNSCKAEAELMLES GGGSIINIASMSGIIVNRGLDQAHYNCSKAGVIHLSKSL AMEWVGKGIRVNSISPGYTATPMNTRPEMVHQTREF ESQTPMQRMAKVEEMAGPALFLASDAASFCTGVDLV VDGGFVCW
OG5_166258	KPNJ1_04170	Endopeptidase CDS	MSRLAAIISAIVICLVVCLGWLASHYHDNATEFKRQRD KATEQLSLAKDTIADMQTRQREVAALDAKYTKELADA KAENDALQRKLDNGGRVLVKGKCPVSASTQTAGAPS MGDDATVELSSVAGRNVLGIRAGIQRDQTALKTLQEY INTQCN
OG5_162799	KPNJ1_04047	Phosphohydrolase (mutt/nudix family protein) CDS	MSAMKMIIIAAAIITDSQGRCLLVRKRGTEYFMQPGGK PEIGETPHAALIRELEEELNFSVSPEELVQVGRFTDAA ANEPGHLVSADVFLIATNRVSFTPTMEIEEVIWFTPGQ DRHIKLAPLTENHLLPLLKGV
OG5_230330	KPNJ1_04195	Exonuclease CDS	MTPEIILERTGIDVTRVEQGDESWHRLRLGVITASEVH NVISKPKSGKKWTDMKMSYFLTLLAEVCTGVAPEVNA KALAWGKQYEADARTLFEFTTDVKVTESPILFRDEGM RTACSPDGLCSDGRGLELKCPFTSRDFMKFRLGGFE AIKSAYMAQVQFSMWVTGKDAWYFANYDPRMKREGI HHVVVERDDKYMSDFNEMVPEFISKMDESLAEIGFTF GEQWK
OG5_129618	KPNJ1_01448	Adenine-specific methyltransferase CDS	MSGKYTLIYADPPWAYRDKAADGDRGAGFKYPVMNV LDICRLPVWELAAEDCLLAMWWVPTQPVEALKVMEA WGFRLMTMKGFTWHKTNKHKGNSAIGMGHMTRANS EDCLFAVRGKLPARMDASICQHVTAPRLENSRKPDVI REKLVQLLGDVPRIELFARQSSHGFDVWGNQCSSPA VELLPGCAVPVVKTEAA
OG5_232878	KPNJ1_04900	HNH endonuclease family protein CDS	MRASSHLFSCQCNAMPSSTTLQHAIENITIWRKGEQR APHKPLLLLYVLSQYQRGHARMFDYASEIRDELHSLL ERFGPQRRQYRPDMPFWRLKGDGFWELHNSEQCSI QGSRKPPGKELELCHVAGGFDEPHFALLNRNKRLINT LAHQILEAHFPESIQEELAEEMGFDLLQIRKERDPHFR QQVLRAYNYECAICGFNMRHDNTSVALEAAHIKWKQ HGGPCEIPNGLALCAIHHKAFDKGSIGLDEDMRIQVSP AVNGGGIVGRLFWDFDGKPITLPQGKECYPQEGFVA WHRREVFRG
OG5_163095	KPNJ1_04906	Superfamily I DNA helicase and helicase subunits CDS	MEKLNALGIVTMLVNRVHSKIVIGDEGLLCIGSFNWFS ATRDEKYKRYDTSMVYRGESLQAEIKTIYSSLEQRKL

OG5_193454	KPNJ1_00475	DNA primase *TraC* CDS	MKMKNAPNIKFLPKDKFTEAIIFAGEDAYSHVQHWIES EGKRAWDDVPPVYLGKRQLAELERLNIVDNGRRSVR VIRAGELSEMQISTIATKLALADVKEARLFNGMFEPQP KEDWTGRLPRLKEEAERGESIVVNLPVKKREPKPEPG DELKPRVESRSDGLYWITPKVDKDSGEIINNETWLCS PLEVVGSGSDGAERYLVLRWRSPRGHEDITRAIPCAD IGERDGWRSLKAGGVNVTTKSTFRAILADWLQQSGT DREWIITHTTGWHHGAYIMPDGEVIGDPETPILFNGRS AASSGYAIAGTAATWRDSVARLAGGNPSMMLGVAAA LSAPLIGLVGADGFGVHLFEQSSAGKTTTANIASSLW GEPDALRLTWYGTALGIANEAEAHNDSLLPLDEVGQG SSAKDVATSAYTLFNGAGKLQGAKEGGNRELKRWRT VAISTGEMDIETFLAAGGLKVKAGQLVRLLNIPMEKST AFNGLPNGKAHADALKEAWIDNHGAAGREWVKWLA ANQQEAKQAVRDAQTRWRGLIPADYGEQVHRVAER FAILEAALVTGASITGWSEQASRDAIQHSFNAWVKEF GTGNKEHQQIIEQCEAFLNAYGLSRFAPLPYDPSSMPI RDLAGYRKRKSSHDDAPLVFYTFPATFEKEIAQGFNA RQFARVLAAAGLLSEPSSGRGYQQKSPRIDGRQINVY VLHQVAEGGEE
OG5_198636	KPNJ1_00605	Tagatose-6-phosphate kinase *GatZ* CDS	MKDIITRHKSGEHIGICSVCSAHPLVIEAALRFDLSTNN KVLIEATSNQVNQFGGYTGMQPADFRDFVYNIARTVG FPAERIILGGDHLGPNCWQDEPAAVAMEKSIDLIKAYV AAGFSKIHLDASMSCADDPVPLDPGVVAERAARLCQ AAEETASDEQKRHLTYVIGTEVPVPGGEASTIGSVHV TRAQDAAATLETHEAAFRKLGLDAALERVIAIVVQPGV EFDHTQIIHYQPQEAKALSAWIESTPMVYEAHSTDYQ TRQAYRALVRDHFAILKVGPALTFALREAIFALAQMEN ELIAPESRSRVMEVIDEVMLNEPGYWKKYYRPTWSQ AMVDIHFSLSDRIRYYWPHPRIRQSVEKLIANLTDAKL PLGLISQYMPVQFERLSLNELNAEPHALILDKIQDVLR AYRYGCSSETA

Supplemental Table 3 – 26 proteinase OGs present in both, KP35 and NJST258-1 but absent in ATCC 43816 KPPR1

KP35 and NJST-258-1 shared 150 OGs that were absent in ATCC KPPR1 and encompass the major differences between the US predominant ST258 and the ST493 ATCC 43816 KPPR1 strain. Notably, 26 out of these 150 OGs are proteinases. There were another 51 OGs consisting of functional proteins related to metabolism, motility, restriction-modification system, or antibiotic resistance. The remainder (73 OGs) were phage-related or hypothetical proteins. These included an antibiotic-induced protein, *drp35*, (KPNJ1_00605), which was shared by KP35 and NJST258 but absent in ATCC 43816 KPPR1. The *drp35* was thought to be specific to *S. aureus* and was shown to be inducible after exposure to cell wall active antibiotics (Murakami, et al., 1999).

Supplemental Table 4

OG group numbers	Representative Protein in the OG	Annotation	Protein seq
OG5_137650	KPNJ1_04021	Transposase CDS	MAKPKYSPETKLAVVNHYLSGKDGEQSTADLFGIERTS VRRWVRAWQFHGAEGLTAKNNHYSDEFKLVVVRAVIS DRLTMREAAARFNLSAEILVRRWLDVYNDAGAEGLLNI QCGRPGKMTKPKNIPPLTDKELEKLSPEELRAELRYLR AENAYLKKLKALVQSEKNGKKP
OG5_137048	KPNJ1_01908	Reverse transcriptase CDS	MERRSGAKGNAEQPHMRRTQSRESMSQRLSRVREAA KQRKKERFTALFHLLTVEALEAAFLSLSRKAAAGVDGIR WMDYAGNMKNNITDLHRRLHQGSYRAQPGRRHYIPKA DGKQRPLGIASLEDKIVQYALVKILNAVYENDFMGFSYG FRPGRSQHDALDALATGLVRTNVNWVLDADISQFFDRV SHEWLIRFTEHRIGDRRVIRLIRKWLTAGTSEEGQWRAT EEGTPQGAVISPLLANIYLHYVFDLWAHQWRRRYATGN VVMVRYADDIVIGFDKRYDARRFRIAMQQPETFNFLGFT HISGKDRNGRFMLIRKTRRDRMTATLKAIKDGLRRRWH YSIPEQGKWLRRVVQGYLNYHSVPGNFPTMQKFRTHV TNLWRRALRRRSQKDDTTWTKANKLAAAWLPRVRVLH PWPVERFTARHPRQEPGA
OG5_135482	KPNJ1_01498	Endochitinase CDS	MDINEFQKAAGVSLALATRWHPHIVAAMKEFGIIKPLDQ AMFIAQAGHESTGFTQLVESFNYSVAGLAGFVRAGRLT QGQANSLGRRQGEPSLPLERQRAIANLVYSKRMGNNG PTDGWFYRGRGLIQTTGLNNYRDCGAALKVDMVKQPE LLAQDDYAARSAAWYFVKYGCLKYTDDLMRVTQIINGG QNGIDDRRVRYLSAKKVLAS
OG5_134231	KPNJ1_03596	Selenate reductase chain *YnfG* CDS	MTTQYGFFIDSARCTGCKTCELACKDYKNLTPEVSFRRI YEYAGGDWQEDNGVWQQNVFAYYLSIACNHCEDPAC TKVCPSGAMHKREDGFVVVNEEVCIGCRYCHMACPYG APQYNADKGHMTKCDGCHERVAEGKKPICVESCPLRA LDFGPIAELRAKHGQLAAVAPLPSAHFTRPSIVIKPNANA RPCGDTTGYLANPKEV
OG5_128670	KPNJ1_01905	Transposase CDS	MAKPKYSPETKLAVVNHYLSGKDGEQSTADLFGIERTS VRRWVRAWQFHGAEGLTAKNNHYSDEFKLVVVRAVIS DRLTMREAAARFNLSAEILVRRWLDVYNDAGAEGLLNM QCGRPGQMTKPKNIPPLTDKELEKLSPEELRAELRYLR AENAYTKKVESLGSERKKWQKALIISELRHEHALRDLLR AAGMSRSTWYYNMNALKQGDRYAGLKENIRKIYHYHK GRYGYRRITLALRKQGLRINHKTVQRLMAELSLRSVIRA KKYRAWKGRTGEAAPNILSRNFGASKANEKWVTDVTE FPVQGKKLYLSSVLDLFNREVIAYSLSERPVMEMVNTM LDGAFPKLRPGDAPLLHSDQGWHYRMRSYQERLKAH GMTQSMSRKGNCLDNAVMENFFGTLKSECFYLREFRS VSALRKAVEDYIHYYNNERISLKLKGLSPVEYRTQALRA A

Supplemental Table 4 – OGs lacking in KP35 but present in the ATCC KPPR1 and NJST258-1 strains
In addition, KP35 was lacking 18 OGs, which were present in both ATCC KPPR1 and NJST-258-1. Five of these 18 OGs were proteinases, including the reverse transcriptase KPNJ1_01908, endochitinase KPNJ1_01498, and selenate reductase chain *ynfG* (KPNJ1_03596). The KPNJ1_01498 is thought to be involved in the cell wall macromolecule catabolic process. KPNJ1_03596 is important for selenate reductase activity which reaction product was selenite. An additional six functional OGs included KPNJ1_05356 (Transporter, drug/metabolite exporter family protein), Transcriptional regulator KPNJ1_00338 and electron transport complex protein *rnfC* CDS KPNJ1_02503, and the remaining 7 OGs were hypothetical proteins. The lack of these proteinases and functional proteins might affect many aspects of the KP35 metabolism and cell wall catabolic process.

Supplemental Table 5

Identified Protein	Molecular Weight (kDa)	KPPR1	KP35	PBS
Serum albumin Alb	69	2800	1829	2520
Complement C3 C3	186	853	815	450
Cluster of Serotransferrin Tf (Q921I1|TRFE_MOUSE)	77	765	690	796
Cluster of Murinoglobulin-1 Mug1 (P28665|MUG1_MOUSE)	165	270	676	293
Cluster of Alpha-2-macroglobulin A2m (Q61838|A2M_MOUSE)	166	206	566	119
Lactotransferrin Ltf	78	375	563	33
Alpha globin 1 haemaglobin alpha 2	15	233	542	165
Cluster of Beta-globin Hbbt1 (A8DUK4|A8DUK4_MOUSE)	16	375	529	263
Cluster of Alpha-1-antitrypsin 1-5 Serpina1e (Q00898|A1AT5_MOUSE)	46	458	478	556
Serine protease inhibitor A3K Serpina3k	47	406	448	335
Cluster of Actin, cytoplasmic 1 (Fragment) Actb (E9Q5F4|E9Q5F4_MOUSE)	29	284	372	335
Cluster of Ceruloplasmin Cp (E9PZD8|E9PZD8_MOUSE)	124	362	349	184
Hemopexin Hpx	51	370	329	215
Alpha-1-antitrypsin 1-1 Serpina1a	49	320	321	372
Plasminogen Plg	91	237	289	173
Serine protease inhibitor A3M Serpina3m	47	212	270	174
Cluster of Serine (Or cysteine) peptidase inhibitor, clade A, member 3N, isoform CRA_a Serpina3n (G3X8T9|G3X8T9_MOUSE)	47	207	249	75
Histone H4 Hist1h4a	11	74	233	9
Cluster of Histone H2A Hist1h2al (F8WIX8|F8WIX8_MOUSE)	14	37	232	3
Fibrinogen beta chain Fgb	55	90	229	36
Cluster of Histone H1.4 Hist1h1e (P43274|H14_MOUSE)	22	46	202	1
Myosin-9 Myh9	226	175	199	165
Neutrophilic granule protein Ngp	19	156	194	10
Gelsolin Gsn	86	148	186	206
Vitamin D-binding protein Gc	54	218	171	118
Alpha-2-HS-glycoprotein Ahsg	37	145	170	133
Cluster of Chitinase-like protein 3 Chil3 (O35744|CHIL3_MOUSE)	44	179	168	75
Cluster of Complement factor H Cfh (E9Q8I0|E9Q8I0_MOUSE)	141	156	163	54
Haptoglobin Hp	39	301	162	143
Cluster of Complement C2 C2 (B8JJN2|B8JJN2_MOUSE)	70	190	162	81
Cluster of Kininogen-1 Kng1 (O08677|KNG1_MOUSE)	73	137	146	110
Cluster of Inhibitor of carbonic anhydrase Ica (Q9DBD0|ICA_MOUSE)	77	128	145	113
Cluster of Inter alpha-trypsin inhibitor, heavy chain 4 Itih4 (E9PVD2|E9PVD2_MOUSE)	105	148	141	43
Transketolase Tkt	68	72	140	45
Cluster of Peroxiredoxin-6 Prdx6 (D3Z0Y2|D3Z0Y2_MOUSE)	22	145	139	274
Transthyretin Ttr	16	84	137	146
Cluster of Alpha-actinin-4 Actn4 (P57780|ACTN4_MOUSE)	105	96	135	110
Beta-actin-like protein 2 Actbl2	42	98	133	128
Cluster of Selenium-binding protein 1 Selenbp1 (P17563|SBP1_MOUSE)	53	209	132	402
Fibrinogen gamma chain Fgg	50	72	130	30

Myeloperoxidase Mpo	81	101	129	0
Cluster of Filamin, alpha Flna (B7FAU9|B7FAU9_MOUSE)	280	107	127	105
Cluster of Tubulin beta-5 chain Tubb5 (P99024|TBB5_MOUSE)	50	211	126	276
Cluster of Moesin Msn (P26041|MOES_MOUSE)	68	194	125	239
Cluster of Histone H2B type 1-H Hist1h2bh (Q64478|H2B1H_MOUSE)	14	35	124	0
Cluster of Talin-1 Tln1 (P26039|TLN1_MOUSE)	270	103	120	255
Pyruvate kinase PKM Pkm	58	108	119	139
Apolipoprotein A-I Apoa1	31	161	117	176
Complement C5 C5	189	89	117	184
Complement component C8 alpha chain C8a	66	54	117	45
MCG140354 Sec14l3	46	191	116	280
Epidermal growth factor receptor Egfr	135	64	116	54
Protein S100-A9 S100a9	13	38	114	2
Cluster of Plastin-2 Lcp1 (Q61233|PLSL_MOUSE)	70	78	114	23
Cluster of Adenylyl cyclase-associated protein 1 Cap1 (P40124|CAP1_MOUSE)	52	66	113	54
Complement C4-B C4b	193	101	111	42
Actin, cytoplasmic 2 (Fragment) Actg1	12	75	110	84
Cluster of Clusterin Clu (Q06890|CLUS_MOUSE)	52	113	109	54
Beta-2-glycoprotein 1 Apoh	39	71	107	63
Annexin A1 Anxa1	39	39	106	9
Complement component C8 beta chain C8b	66	49	104	35
Cluster of Carboxylesterase 1C Ces1c (P23953|EST1C_MOUSE)	61	97	103	134
Cluster of Alpha-enolase Eno1 (P17182|ENOA_MOUSE)	47	77	103	106
Thrombospondin 1 Thbs1	130	39	101	1
Inter-alpha trypsin inhibitor, heavy chain 2 Itih2	106	23	97	32
Cluster of Heat shock cognate 71 kDa protein Hspa8 (P63017|HSP7C_MOUSE)	71	102	95	161
Cluster of Fibronectin Fn1 (A0A087WR50|A0A087WR50_MOUSE)	263	110	91	29
Ig mu chain C region (Fragment) Ighm	50	15	90	9
Neutrophil gelatinase-associated lipocalin Lcn2	23	95	87	11
Chitinase-3-like protein 1 Chi3l1	44	208	85	108
Cluster of Antithrombin-III Serpinc1 (P32261|ANT3_MOUSE)	52	85	84	146
Cluster of 14-3-3 protein zeta/delta Ywhaz (P63101|1433Z_MOUSE)	28	129	81	162
Inter-alpha-trypsin inhibitor heavy chain H1 Itih1	102	29	81	23
Cluster of Coronin-1A Coro1a (O89053|COR1A_MOUSE)	51	29	79	0
Cluster of Tubulin alpha-1B chain Tuba1b (P05213|TBA1B_MOUSE)	50	131	76	207
Histone H1.5 Hist1h1b	23	10	76	0
Cluster of Leukocyte elastase inhibitor A Serpinb1a (Q9D154|ILEUA_MOUSE)	43	31	75	2
Complement factor I Cfi	67	60	74	54
Cluster of Fructose-bisphosphate aldolase Aldoa (A6ZI44|A6ZI44_MOUSE)	45	53	73	69
Cluster of Glyceraldehyde-3-phosphate dehydrogenase Gm3839 (S4R1W1|S4R1W1_MOUSE)	36	70	73	101
Serine protease inhibitor A3C Serpina3c	47	68	73	61
Fibrinogen alpha chain Fga	87	58	72	13
Glycogen phosphorylase, liver form Pygl	97	26	71	6
Cluster of Tropomyosin alpha-3 chain Tpm3 (E9Q7Q3|E9Q7Q3_MOUSE)	29	99	69	120

Carbonic anhydrase 2 Ca2	29	54	67	50
Afamin Afm	69	45	66	47
Heat shock protein HSP 90-alpha Hsp90aa1	85	64	66	135
Superoxide dismutase [Cu-Zn] Sod1	16	70	65	47
Oxidation resistance protein 1 C7	93	44	64	31
6-phosphogluconate dehydrogenase, decarboxylating Pgd	53	34	64	34
Vitronectin Vtn	55	30	64	32
High mobility group protein B2 Hmgb2	24	20	63	7
Plasma kallikrein Klkb1	71	28	62	19
Leukotriene A-4 hydrolase Lta4h	69	47	62	11
Vinculin Vcl	117	86	60	172
Dihydropyrimidinase-related protein 2 Dpysl2	62	133	60	228
Cluster of Vimentin Vim (P20152|VIME_MOUSE)	54	25	60	2
78 kDa glucose-regulated protein Hspa5	72	27	60	23
Cluster of Elongation factor 1-alpha 1 Eef1a1 (P10126|EF1A1_MOUSE)	50	72	59	106
Pulmonary surfactant-associated protein D Sftpd	38	86	59	63

Supplemental Table 5 – Top 100 proteins from proteomic analysis
Shotgun proteomics of pooled BALF (N=3) recovered with KPPR1 (10^5 CFU) and KP35 (10^6 CFU) infected mice after 48 hours. Equivalent inocula recovered (10^6 CFU) at this time point despite disparate inocula administered (10^6 CFU). Top absolute protein levels from LC-MS/MS analysis of BALF from KP35 and congruent levels in PBS control and KPPR1 infected mice.

Supplemental Videos

Supplemental Video 1 – Differential activation of Ca^{2+} fluxes in neutrophils exposed to KPPR1 versus KP35 Calcium fluxes were measured by fluorescence activation on an inverted microscope with a GFP mercury laser. Murine neutrophils loaded with AM/Fluo-4 1mM and PowerLoad concentrate 1mM, 2 hours prior to stimulation with (A) KP35 or (B) KPPR1 (MOI 100) or (C) media alone followed by thapsigargin (1µM) (T) as a positive control (added halfway through). Video is a compilation of representative images from 3 independent experiments. For bacterial infections, each frame is 20 sec apart over a 20-minute period and for media alone followed by thapsigargin 20 sec apart over a 30-minute period.

METHODS

Antibodies and Inhibitors. Antibodies used in vivo were administered intraperitoneally (i.p). Neutrophil depletion was accomplished with InVivoMAb (BioXCell) anti-Ly6G/C (RB6-8C5) 250 µg, anti-Ly6G (1A8) 500 µg, and isotype control anti KLH; Rat IgG 2b (LTF-2) 250 µg. Antibody used to block TNFR2 activity was LEAF (Biolegend) purified anti-mouse CD120b (TNFR type II/p75) (TR75-54.7) compared to isotype control purified Armenian Hamster IgG Isotype Control (HTK-8888). Antibodies used to block CCR2 were a kind gift from Matthias Mack, Universitätsklinikum Regensburg, Regensburg, Germany {Schumak:2015cp}, clone MC-21 hybridoma with isotype control (MC-67, rat IgG2b κ). For Western blot, the following antibodies were utilized pSTAT1 (abcam, phospho Y701, ab30645), STAT1 (Cellsignaling, pSTAT3 (Cellsignaling), STAT3 (Cellsignaling), and actin (Sigma).

Mouse studies. In vivo experiments were performed using 8 week old, male C57BL/6J mice (Jackson Laboratories). Mice were anesthetized with 100 mg/kg ketamine and 5 mg/kg xylazine given i.p. and infected intranasally with KP35 (10^8 CFU in 50 µL of PBS) or KPPR1 (10^2 CFU in 50 µL of PBS), and sacrificed 4-96 hours after infection. When KP35 infection was compared to *P. aeruginosa* PAK, a lower and equivalent inocula was administered (10^7 CFU in 50 µL of PBS) for a 24 hour infection. To deplete macrophages, 75 µL of clodronate loaded liposomes or PBS liposome controls were inoculated intranasally 24 hours prior to infection as previously described (Martin, Parker, Harfenist, Soong, Prince, 2011). For the competitive index experiment, mice were inoculated intranasally with 10^8 CFU at a 1:10 ratio of NR1155:KP35 or 10^7 CFU at a 1:1. Bacterial load of each compartment was quantified by serial dilutions on enriched agar. Animal experiments were performed in accordance with the guidelines of the IACUC at Columbia University (protocol number AAAG9307) or the Bioethics and Biosafety Committee of the Pontificia Universidad Católica de Chile (CEC 150721005).

Analysis of immune cell populations. For the clodronate depletion experiment, analysis of cell populations in BALF or single cell suspension of lung homogenate was conducted using a BD Calibur as previously described (Parker, et al., 2011). Cells were labeled with a combination of phycoerythrin (PE)-labeled anti-NK 1.1 (PK136; eBioscience), fluorescein (FITC)-labeled anti-Ly6G/C (RB6-8C5; eBioscience), allophycocyanin (APC)-labeled anti-MHCII (M5/114.15.2; eBioscience), PerCP-Cy5.5-labelled anti-CD11c (N418; Biolegend). In this experiment alone, neutrophils (NEUTs) were defined as $Ly6G^+/MHCII^-$ and macrophages/monocytes as $CD11c^+/MHCII^{low\text{-}mid}$.

Bone marrow MDSC (BM/MDSC) differentiation and infection. BM/MDSCs were differentiated as previously described**,** with some modifications (Marigo, Bosio, Solito, Mesa, Fernandez, Dolcetti, Ugel, Sonda, Bicciato, Falisi, Calabrese, Basso, Zanovello, Cozzi, Mandruzzato, Bronte, 2010). Briefly, 5 x 10^6 bone marrow cells were seeded into 100 mm dishes in 10 mL of RPMI 1640 2 mM L-glutamine, 10 mM HEPES, 20 µM 2-ME, 1% streptomycin/penicillin, and 10% heat-inactivated FBS supplemented with GM-CSF (40 ng/mL) and G-CSF (40 ng/mL) (Peprotech). Cells were maintained at 37ºC and 5% CO_2 for 5 days. On day 5, cells were washed twice and resuspended in RPMI 1640 + FBS 10%. An aliquot of cells were stained by flow cytometry before and after differentiation. To evaluate the cytokine production by the BM/MDSCs, $1x10^5$ cells/well were seeded into 48-wells plate and stimulated with PBS, LPS (1µg/mL), or opsonized KP35 (MOI 10) for 4 hours at 37ºC and 5% CO_2. Cytokine production was measured in the cell culture supernatant by 31-plex mouse discovery assay (Eve Technologies). To evaluate the bactericidal capacity of the BM/MDSCs, $1x10^5$ cells were seeded into 96-wells plate and stimulated with $1x10^5$ CFU (MOI 1) of opsonized KPPR1 or KP35 for 0, 1, 2 and 4 hours at 37ºC with 5% CO_2. Cell viability was measured by counting total cell number in a conventional hemocytometer with trypan exclusion, whereas bacterial viability was measured by serial dilutions plated after cell lysis with saponin 1%. Additional cells were stimulated with KPPR1 or KP35 (MOI 10) for gene expression analysis by qRT-PCR.

REFERENCES

1. Poe SL, Arora M, Oriss TB, et al. STAT1-regulated lung MDSC-like cells produce IL-10 and efferocytose apoptotic neutrophils with relevance in resolution of bacterial pneumonia. *Mucosal Immunol.* Jan 2013;6(1):189-199.
2. Tzouvelekis LS, Miriagou V, Kotsakis SD, et al. KPC-producing, multidrug-resistant *Klebsiella pneumoniae* sequence type 258 as a typical opportunistic pathogen. *Antimicrob Agents Chemother.* Oct 2013;57(10):5144-5146.
3. Martin FJ, Parker D, Harfenist BS, Soong G, Prince A. Participation of CD11c(+) leukocytes in methicillin-resistant *Staphylococcus aureus* clearance from the lung. *Infect Immun.* May 2011;79(5):1898-1904.
4. Misharin AV, Morales-Nebreda L, Mutlu GM, Budinger GR, Perlman H. Flow cytometric analysis of macrophages and dendritic cell subsets in the mouse lung. *Am J Respir Cell Mol Biol.* Oct 2013;49(4):503-510.
5. Penaloza HF, Nieto PA, Munoz-Durango N, et al. Interleukin-10 plays a key role in the modulation of neutrophils recruitment and lung inflammation during infection by *Streptococcus pneumoniae*. *Immunology.* Sep 2015;146(1):100-112.
6. Marigo I, Bosio E, Solito S, et al. Tumor-induced tolerance and immune suppression depend on the C/EBPbeta transcription factor. *Immunity.* Jun 25 2010;32(6):790-802.
7. Xiong H, Carter RA, Leiner IM, et al. Distinct Contributions of Neutrophils and CCR2+ Monocytes to Pulmonary Clearance of Different *Klebsiella pneumoniae* Strains. *Infect Immun.* Sep 2015;83(9):3418-3427.
8. Polz J, Remke A, Weber S, et al. Myeloid suppressor cells require membrane TNFR2 expression for suppressive activity. *Immun Inflamm Dis.* Aug 2014;2(2):121-130.
9. Hu X, Li B, Li X, et al. Transmembrane TNF-alpha promotes suppressive activities of myeloid-derived suppressor cells via TNFR2. *J Immunol.* Feb 1 2014;192(3):1320-1331.
10. Schumak B, Klocke K, Kuepper JM, et al. Specific depletion of Ly6C(hi) inflammatory monocytes prevents immunopathology in experimental cerebral malaria. *PLoS One.* 2015;10(4):e0124080.
11. Murakami H, Matsumaru H, Kanamori M, Hayashi H, Ohta T. Cell wall-affecting antibiotics induce expression of a novel gene, drp35, in *Staphylococcus aureus*. *Biochem Biophys Res Commun.* Oct 22 1999;264(2):348-351.
12. Parker D, Martin FJ, Soong G, et al. *Streptococcus pneumoniae* DNA initiates type I interferon signaling in the respiratory tract. *MBio.* 2011;2(3):e00016-00011.